OXFORD

SOT | Society of Toxicology
www.toxsci.oxfordjournals.org

TOXICOLOGICAL SCIENCES, 151(1), 2016, 57–70

doi: 10.1093/toxsci/kfw022
Advance Access Publication Date: February 10, 2016
Research Article

Estimating Margin of Exposure to Thyroid Peroxidase Inhibitors Using High-Throughput *in vitro* Data, High-Throughput Exposure Modeling, and Physiologically Based Pharmacokinetic/ Pharmacodynamic Modeling

Jeremy A. Leonard,[*,†] Yu-Mei Tan,[†] Mary Gilbert,[‡] Kristin Isaacs,[†] and Hisham El-Masri[‡,1]

[*]Oak Ridge Institute for Science and Education, Oak Ridge, Tennessee, 37831; [†]National Exposure Research Laboratory, United States Environmental Protection Agency, Research Triangle Park, North Carolina, 27709; and [‡]National Health and Environmental Effects Research Laboratory, United States Environmental Protection Agency, Research Triangle Park, North Carolina, 27709

[1]To whom correspondence should be addressed at National Health and Environmental Effects Research Laboratory, United States Environmental Protection Agency, 109 T.W. Alexander Dr Mail Code B105-03, Research Triangle Park, North Carolina 27709. Fax: 919-541-1302. E-mail: el-masri.hisham@epa.gov.

ABSTRACT

Some pharmaceuticals and environmental chemicals bind the thyroid peroxidase (TPO) enzyme and disrupt thyroid hormone production. The potential for TPO inhibition is a function of both the binding affinity and concentration of the chemical within the thyroid gland. The former can be determined through *in vitro* assays, and the latter is influenced by pharmacokinetic properties, along with environmental exposure levels. In this study, a physiologically based pharmacokinetic (PBPK) model was integrated with a pharmacodynamic (PD) model to establish internal doses capable of inhibiting TPO in relation to external exposure levels predicted through exposure modeling. The PBPK/PD model was evaluated using published serum or thyroid gland chemical concentrations or circulating thyroxine (T_4) and triiodothyronine (T_3) hormone levels measured in rats and humans. After evaluation, the model was used to estimate human equivalent intake doses resulting in reduction of T_4 and T_3 levels by 10% (ED_{10}) for 6 chemicals of varying TPO-inhibiting potencies. These chemicals were methimazole, 6-propylthiouracil, resorcinol, benzophenone-2, 2-mercaptobenzothiazole, and triclosan. Margin of exposure values were estimated for these chemicals using the ED_{10} and predicted population exposure levels for females of child-bearing age. The modeling approach presented here revealed that examining hazard or exposure alone when prioritizing chemicals for risk assessment may be insufficient, and that consideration of pharmacokinetic properties is warranted. This approach also provides a mechanism for integrating *in vitro* data, pharmacokinetic properties, and exposure levels predicted through high-throughput means when interpreting adverse outcome pathways based on biological responses.

Key words: thyroid peroxidase; adverse outcome pathway; margin of exposure; PBPK/PD model; high-throughput *in vitro* assay.

Published by Oxford University Press on behalf of the Society of Toxicology 2016.
This work is written by US Government employees and is in the public domain in the US.

The utility of the Adverse outcome pathway (AOP) framework lies in its ability to provide a biological context for facilitating the interpretation of data from high-throughput (HT) *in vitro* assays (Tollefsen *et al.*, 2014). The AOP framework rests on the assumption that multiple chemicals can act through a common biological pathway that leads to a specific adverse outcome, such that chemical interactions with a specific molecular target identified in HT assays can be linked to health consequences for a whole organism or population (Ankley *et al.*, 2010; Edwards *et al.*, 2015). Although the coupling of an AOP with HT testing is useful for prioritizing chemicals in lower tier hazard assessment, higher tier risk assessment requires quantitative linkages between external exposure levels to internal doses able to perturb the molecular target (Groh *et al.*, 2015). These linkages require the understanding of exposure pathways and pharmacokinetics (PKs) (absorption, distribution, metabolism, and excretion [ADME]). In data-poor situations, considering these pathways/processes qualitatively can aid in refining HT findings through identification of false positives (ie, *in vitro* active chemicals incapable of reaching the molecular target) and false negatives (ie, parents of active metabolites or *in vivo* active chemicals unable to be detected *in vitro*) (Phillips *et al.*, 2016). In data-rich situations, computational models can be used to predict exposure doses and track chemical disposition in a biological system, allowing for the linking of an *in vivo* target tissue/blood concentration expected to perturb the molecular target, as identified through *in vitro* testing, to an external exposure level (*in vitro* to *in vivo* extrapolation [IVIVE]).

Such an IVIVE approach was applied by Judson *et al.* (2011) to estimate conazole fungicide concentrations sufficient enough to significantly alter the xenobiotic constitutive androstane receptor/pregnane X receptor signaling pathway *in vivo*. In their study, *in vitro* concentration–response relationships were used to derive a biological pathway altering concentration in blood at steady state. This blood concentration was then converted to a biological pathway-altering dose (BPAD) using a one compartment PK model assuming 100% oral bioavailability, and having only 2 ADME-related parameters, intrinsic clearance and fraction of the chemical unbound to plasma proteins (Judson *et al.*, 2011). The BPAD for each fungicide was then compared with chronic exposure levels from food residues for HT risk assessment. When chemical-specific exposure or ADME data are lacking, such an approach is used mainly for chemical prioritization due to the uncertainties inherent in the accuracy of HT data or predictions.

On the other hand, when exposure and ADME data are sufficient, the IVIVE approach can be applied to estimate a margin of exposure (MOE) for assessing risk for individual chemicals. In the present a framework was constructed to apply the IVIVE approach. The AOP selected for use as a case study was the inhibition of thyroid peroxidase (TPO), a key synthesis enzyme for thyroid hormone production in the thyroid gland. This framework involved the integration of HT *in vitro* data targeting thyroid disruption, a physiologically based pharmacokinetic/pharmacodynamic (PBPK/PD) model that simulates changes in serum thyroid hormone levels following chemical exposures, and estimation of environmental exposure levels (either from literature or HT models) to estimate MOEs. Specifically, (1) a PBPK model was developed to predict target tissue (ie, the thyroid gland) dosimetry; (2) the PBPK model was coupled with a PD model to estimate a human equivalent oral dose as a function of target tissue dose and HT *in vitro* data for TPO inhibition; and (3) human equivalent doses and estimated environmental exposure levels were used to calculate a MOE for 6 potential TPO inhibitors. Although only 1 specific AOP is presented in this case study, the utility of this integrated framework lies in its versatility in being able to investigate multiple chemicals across various AOPs. This case study also highlights the value of chemical-specific exposure and ADME data when applying the integrative framework in chemical prioritization or risk-based decision making.

METHODS

Framework overview

Our framework integrated HT *in vitro* hazard data, literature-reported or HT *in silico* model-predicted exposure levels, and chemical-specific ADME characterization to prioritize chemicals based on distance between an intake equivalent dose expected to perturb a molecular target and an environmental concentration to which a population would likely be exposed. These individual components of the integrated framework (illustrated in Figure 1) are discussed in detail in following subsections. A case study that includes 6 chemicals with varying degrees of potency for TPO inhibition (Paul *et al.*, 2014) was used to demonstrate the application of our framework.

HT in vitro assay

The experimental details for the *in vitro* HT TPO inhibition assay, as adapted from an existing rat thyroid microsome assay, are given in Paul *et al.* (2014). In this study, 6 chemicals were chosen from Paul *et al.* (2014) that ranged in potency from high (methimazole [MMI] and 6-propylthiouracil [PTU]) to moderate (benzophenone-2 [BP2] and 2-mercaptobenzothiazole [MBT]) to weak (triclosan [TCS] and resorcinol [RSC]). The concentration necessary to reduce TPO activity by 50% (IC_{50}) and the maximum inhibitive activity (I_{max}) for each chemical were used as 2 of the inputs into the PD model, which is described below.

PD model

TPO plays a critical role in the synthesis of the thyroid hormones T_4 and T_3 through its conversion of iodide taken up from the blood into iodine by hydrogen peroxide-mediated oxidation (Jameson and Wheetman, 2001). Numerous xenobiotic chemicals have been identified to alter the biosynthesis, secretion, and regulation of thyroid hormones through feedback mechanisms related to the production and release of thyroid stimulating hormone (TSH), T_4, and T_3 (Crofton *et al.*, 2005; Jugan *et al.*, 2010). A quantitative model was developed by Ekerot *et al.* (2013) to predict the effects of TPO inhibitors on thyroid hormone homeostasis in humans. This model was modified in this study (Supplementary Figure S1) to describe changes in serum thyroid hormone (T_3, T_4, and TSH) concentrations in rats and humans following exposures to the 6 selected chemicals (Table 1). In this model, iodine is assumed to be readily available, and chemical effects are related only to TPO inhibition. The inhibitory effect of a chemical on TPO was described in our modified PD model as a function of I_{max}, IC_{50}, (both were obtained from the *in vitro* study [Paul *et al.*, 2014]), and the concentration of the chemical in thyroid tissue over time (C_{Thy}) derived from the PBPK model. Production rates of TSH and T_4 were estimated from degradation rates of the 2 hormones and from their baseline levels in the absence of TPO inhibitors to ensure that TSH and T_4 concentrations in plasma remain at their baseline values in the absence of chemical exposure. A similar approach was taken

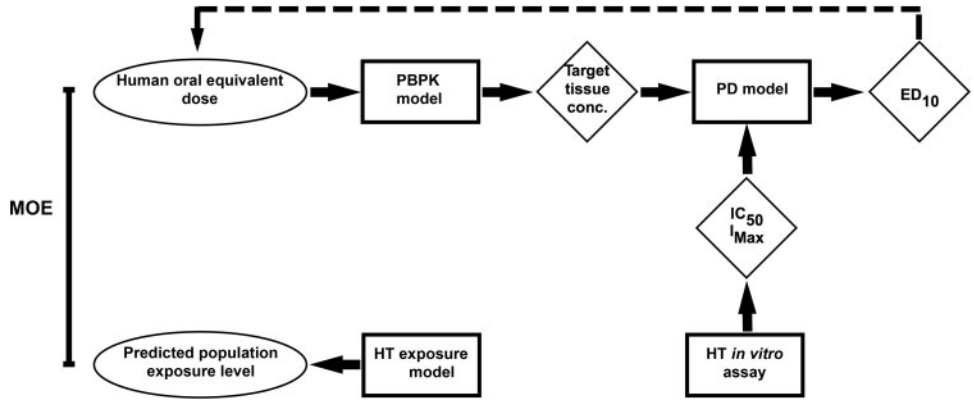

FIG. 1. Workflow of the integrated modeling approach and its individual HT components. Squares represent processes, diamonds represent intermediates used as inputs into the next component, and ovals represent final outputs for decision making. The dashed line represents extrapolation of human equivalent dose from the combined PBPK and PD model.

when estimating T_3 production rates, although in this case, both the minor production of T_3 in thyroid tissue, as well as the more abundant production via peripheral metabolic conversion of T_4 into T_3, were taken into account during model calibration. All other PD model parameters were taken from literature (see references in Table 1).

PBPK model

The PBPK model for rats and humans included 10 perfusion-limited compartments: the thyroid, fat, brain, muscle, skin, kidney, liver, lumen and gastrointestinal (GI) tract, and slowly and rapidly perfused tissues (Supplementary Figure S2). In this PBPK model, only oral ingestion was simulated, as individuals are exposed to the 6 selected chemicals primarily through this route. Chemical-specific tissue-to-blood partition coefficients (PCs) were estimated based on common physicochemical properties (eg, solubility) (Rodgers *et al.*, 2005; Rodgers and Rowland, 2006) through use of the proprietary software GastroPlus (Simulations Plus, Inc., Lancaster, California). As the generic GastroPlus module does not include a thyroid compartment, the same value as that of the kidney-to-blood PC was used for the thyroid lumen-to-blood PC. This approach was taken because the colloid lumen, or the region between the colloid and follicular cells, is the site at which thyroid hormone production occurs (Zoeller et al., 2007). According to a published PBPK model describing perchlorate kinetics in humans, the thyroid-to-blood PC is 0.13 for iodide and 0.15 for perchlorate, while the lumen-to-thyroid PC is 7.0 for both substrates (Merrill *et al.*, 2005). The resulting lumen-to-blood PC is 1.05 for iodide and 0.91 for perchlorate, and these values are most similar to the kidney-to-blood PCs (1.09 for iodide and 0.99 for perchlorate) for all given tissue-to-blood PCs (Merrill *et al.*, 2005).

The oral absorption rate for each chemical (min^{-1}) was estimated from GastroPlus using the following equation:

$$k_a = P_{eff} \times \alpha \quad (1)$$

where α is 2/R and R is the radius of each of the 9 GI compartments simulated in GastroPlus, P_{eff} is the human-equivalent effective jejunal (source of the 9 compartments) permeability coefficient, and k_a is the maximum absorption rate coefficient, as determined by plotting net k_a versus time for the 9 GI compartments in GastroPlus. The initial oral dose was first introduced into the intestinal lumen, followed by the GI tract and liver, before entering into systemic circulation and distributing to body tissues. Physiological parameters used in the rat and human models were obtained from literature (Brown *et al.*, 1997; Tables 2 and 3). The PBPK model was used to determine the concentration of each chemical within the thyroid compartment, and together with the PD model and using reverse dosimetry, the human equivalent intake dose resulting in a 10% reduction in circulating T_4 and T_3 levels due to TPO inhibition (ED_{10}) was estimated. The 10% threshold was considered to be a conservative estimate for minimal adverse health effects according to United States Environmental Protection Agency guidelines (USEPA, 2011). All PBPK/PD model simulations were conducted in MATLAB (version R2014b; The MathWorks, Inc., Natick, Massachusetts).

In addition to PCs, the other critical chemical-specific data required in a PBPK model is the determination of clearance of chemicals. Rather than using 2 distinct clearance terms for urinary excretion and hepatic clearance, one single rate was used to describe the total clearance of the chemical. In our study, total clearance for each chemical was taken as a function of both biological half-life and volume of distribution according to the first order kinetic rate equation:

$$Cl_{Tot} = \frac{\ln(2) \times Vd}{t_{1/2}} \quad (2)$$

where V_d (l/kg) is the volume of distribution, $t_{1/2}$ (h) is the biological half-life, and Cl_{Tot} is the total body clearance (ml/min) for each chemical.

Total clearance for MMI in rats was estimated from recovery of radio-labeled MMI from whole blood samples taken intermittently over 24 h after a single intravenous dosing of 20 mg/kg; the $t_{1/2}$ of decay was 3.85 h, and V_d was 67 ml per 100 g rat BW (Sitar and Thornhill, 1973). Total clearance for PTU in rats was estimated from plasma concentrations of PTU taken intermittently within a 24-h period after a single intraperitoneal dose of 3.3 mg/kg PTU; the $t_{1/2}$ was approximately 6 h, and V_d was 0.73 l/kg (Giles *et al.*, 1982). Total clearance for TCS in rats was estimated from TCS concentrations in recovered plasma samples taken intermittently over a 48-h period after a single oral dose of 5 mg/kg; the $t_{1/2}$ was 48.5 h, and V_d was 73.5 l/kg (Wu *et al.*, 2009).

Total clearance for MMI in humans was calculated based on a V_d of 0.6 l/kg (Hengstmann and Hohn, 1985), approximating a

TABLE 1. Thyroid Hormone[a] Elimination Rates, Generation Rates, Baseline Values, and Slope Parameters Used for the Rat and Human Thyroid Feedback PD Model

Model	Parameter	Value	Units	Source
Rat	T_4 Elimination	9.63E-04	1/min	Modified from Silva et al. (1984)[b]
	T_3 Elimination	9.17E-03	1/min	Modified from Silva et al. (1984)[b]
	T_4 Generation	4.04E-03	ug/dl/min	Modified from Ekerot et al. (2013)[d]
	T_3 Generation	1.70E-06[c]	ug/dl/min	Modified from Ekerot et al. (2013)[d]
	TSH Generation	1.22E-04	ug/dl/min	Modified from Ekerot et al. (2013)[d]
	T_4 Base Line	4.2	ug/dl	Huffman and Hedge (1986)
	T_3 Base Line	95.0	ng/dl	Huffman and Hedge (1986)
	TSH Base Line	5.0	ng/ml	Choksi et al. (2003)
	fr	0.215[c]	unitless	Silva et al. (1984)
Human	T_4 Elimination	7.78E-05	1/min	Nicoloff et al. (1972)
	T_3 Elimination	4.72E-04	1/min	Nicoloff et al. (1972)
	T_4 Generation	7.50E-03	nM/min	Modified from Ekerot et al. (2013)[d]
	T_3 Generation	7.78E-06[c]	nM/min	Modified from Ekerot et al. (2013)[d]
	TSH Generation	3.14E-05	nM/min	Modified from Ekerot et al. (2013)[d]
	T_4 Base Line	96.5	nmol/l	Ridgway et al. (1974)
	T_3 Base Line	3.2	nmol/l	Ridgway et al. (1974)
	TSH Base Line	0.129	nmol/l	Odell et al. (1967)[e]
	fr	0.20[c]	unitless	McGuire and Hays (1981)
	TSH Elimination	2.43E-04	1/min	Ekerot et al. (2013)
For all models	SF1	2.53	unitless	Ekerot et al. (2013)
	SF2	1.90	unitless	Ekerot et al. (2013)
	SF3	0.11	unitless	Ekerot et al. (2013)

[a]T_4, thyroxine, T_3, triiodothyronine, and TSH, thyroid stimulating hormone.
[b]Extrapolated using the results of radiolabelled iodine tracer studies (Oppenheimer et al., 1972).
[c]The 35% reduction in the fractional conversion of T_4 to T_3 caused by 6-propylthiouracil (21.5–14.0% in rats and 20–13% in humans) resulted in a T_3 generation rate of 3.06E-04 in rats and 5.33E-04 in humans. The value provided in the table represents generation of T_3 without this reduced fractional conversion and was used for all chemicals other than 6-propythiouracil.
[d]Generation rates were derived from differential equations used to describe changes in time of TSH, T_4, and T_3 (Equations 3, 6, and 9 of Ekerot et al., 2013). Rather than examining changes in thyroid hormone concentrations, it was assumed that in absence of a chemical dose each respective hormone could be assigned its baseline concentration to simulate steady state.
[e]Assuming 1.5 U/mg and a molecular weight of 14 000 for the active alpha subunit of the TSH hormone, with a baseline concentration of 2.7 uU/ml for eurythyroid individuals (Odell et al. 1967).

total body water volume of 60–65%, and using a $t_{1/2}$ of 6 h (Cooper *et al.*, 1984a). Total clearance for PTU in humans was calculated based on a V_d of 0.42 l/kg (Kampmann and Hansen, 1981) and a $t_{1/2}$ of 1.28 h (Kampmann and Skovsted, 1974). Total clearance for TCS in humans was estimated from measured plasma concentrations over 8 h for individuals given a single oral dose of 4 mg in 13 ml of a mouthwash solution after an overnight fasting period; the median $t_{1/2}$ of TCS was 19 h, and V_d was 1.14 l/kg (Sandborgh-Englund *et al.*, 2006). No literature-reported values of V_d could be obtained for the 3 remaining environmental chemicals, so these values were predicted using the ADMET Predictor (Simulations Plus, Inc., Lancaster, California). Predicted V_d values were 0.8 l/kg, 0.43 l/kg, and 0.25 l/kg for RSC, MBT, and BP2, respectively. The biological half-lives in rats are estimated to be 19 h for BP2 (Jeon *et al.*, 2008), 6 h for MBT (Garcia, 2004), and 10 h for RSC (Merker *et al.*, 1982). Rather than using reported half-lives for rodents, biological half-lives of RSC, MBT, and BPT were estimated from their log *P* values according to the equation of Sarver *et al.* (1997):

$$\log t_{\frac{1}{2}} = 0.452 + 0.288 \times \log P \quad (3)$$

The $t_{1/2}$ values for each chemical, as predicted using the equation above, were 4.65, 13.63, and 12.76 h for RSC, MBT, and BP2, respectively.

After parameterizing the PBPK model, the PBPK/PD model was evaluated by comparing model predictions against time course plasma or thyroid gland concentrations and/or thyroid hormone concentrations for PTU, MMI, and TCS measured in rats. The model-simulated time course concentrations of PTU, T_3, and T_4 in serum, and of PTU in the thyroid gland were compared against measured values in rats (200–250 g body weight [BW]) given 0.05% (0.5 mg/ml) PTU in drinking water for 7 days (Cooper *et al.*, 1983). Assuming consumption of 25 ml drinking water (or approximately 10 ml/100 g) per day, which falls within the normal range of 20–50 ml/d (http://web.jhu.edu/animalcare/procedures/rat.html; Accessed February 19, 2016), the estimated dosage used in the model was 8.7×10^{-6} g/min. In our simulations, no dose was given in the first 2 days in order to demonstrate the persistence of baseline hormone levels. Then, the model was run to simulate daily dosing for 7 days, followed by no PTU dosing for a time sufficient enough to allow hormone levels to return to baseline concentrations. The model was also used to predict MMI concentrations in serum and in the thyroid gland for comparison against MMI concentrations measured in rats given a 0.05% dose in drinking water for 7 days (Cooper *et al.*, 1984b). The third model evaluation case compared model simulations in rats against TCS concentrations in serum measured in rats given a single oral dose of 5 mg/kg in 1 ml corn oil (Wu *et al.*, 2009), serum T_3 and T_4 in male Wistrar rats given daily oral doses of 0–300 mg/kg TCS for 31 days postweaning (Zorrilla *et al.*, 2009), and serum T_3 and T_4 in female young Long-Evans rats given daily oral doses of 0–1000 mg/kg TCS for 4 days (Paul *et al.*, 2010). The only measured human data available for evaluating our PBPK/PD model was of MMI concentrations in serum samples taken over 8 h from individuals that had fasted

TABLE 2. Physiological Parameters Used for the Rat PBPK Model

Parameter	Value	Source
BW (g)- assume 1 g = 1 ml	250.0	Nong et al. (2008)
Cardiac Output (Q_CO; ml/min)	83.0	Brown et al. (1997)
Tissue volume (as a fraction of BW)		
Kidney (V_Kid)	0.0073	Brown et al. (1997)
Liver (V_Liv)	0.0366	Brown et al. (1997)
GI tract (V_GI)	0.0269	Brown et al. (1997)
Rest of body (V_Rap)	0.0137	Brown et al. (1997); remaining tissues
Muscle (V_Mus)	0.404	Brown et al. (1997)
Skin (V_Skin)	0.190	Brown et al. (1997)
Slowly perfused tissues (V_Slow)-for bone	0.050	Brown et al. (1997)
Adipose (V_Fat)	0.064	Brown et al. (1997)
Brain (V_Brn)	0.0057	Brown et al. (1997)
Thyroid (V_Thy)	0.00005	Brown et al. (1997)
Blood (V_Bld)	0.070	Brown et al. (1997)
Blood Flow (as a Fraction of Cardiac Output)		
Kidney (Q_Kid)	0.141	Brown et al. (1997)
Liver (Q_Liv)	0.183	Brown et al. (1997)
Rest of body (Q_Rap)	Difference	Q_CO—blood flow of all other tissues
Muscle (Q_Mus)	0.278	Brown et al. (1997)
Skin (Q_Skin)	0.058	Brown et al. (1997)
Slowly perfused tissues (Q_Slow)- for bone	0.122	Brown et al. (1997)
Adipose (Q_Fat)	0.070	Brown et al. (1997)
Brain (Q_Brn)	0.020	Brown et al. (1997)
Thyroid (Q_Thy)	0.00271	Huffman and Hedge (1986)
Portal vein (Q_PV)	0.153	Brown et al. (1997)
Hepatic artery (Q_HA)	Difference	Q_Liv–Q_PV

overnight and were given a single oral dose of 30 or 60 mg (Cooper *et al.*, 1984a). Time-course serum concentration data from that study was digitized using the UN-SCAN-IT digitizing software (Silk Scientific, Inc., Orem, Utah), and model-predicted MMI concentrations in the blood were then compared against the measured concentrations at both doses.

Sensitivity analyses

The model's system of equations can be written as:

$$\frac{d\vec{x}}{dt} = g\left(\vec{x}, \vec{q}\right) \tag{4}$$

where $\vec{x}$ is the vector state of variables (eg, change in T_4) and $\vec{q}$ is the vector set of the parameters (eg, clearance), and the derivation of the sensitivity equations can be described as:

$$\frac{d}{dq_i}\frac{dx_j}{dt} = \frac{d}{dt}\frac{dx_j}{dq_i} \tag{5}$$

Switching the order of differentiation leads to a system of ordinary differential equations whose state variables (dx_j/dq_i) represent the sensitivity of the model states to each parameter. The formulation of the sensitivity equations was completed using the automatic differentiation package for MATLAB written by Martin Fink and Adam Attarian and available at MATLAB central (http://www.mathworks.com/matlabcentral/; Accessed February 19, 2016). The system of sensitivity equations was integrated with the model equations using MATLAB's ODE solver. The sensitivity coefficients were normalized by dividing the value of the state variable, and multiplying by the parameter for which the derivative was being determined (eg, $\frac{dx_j}{dq_i}\frac{q_i}{x_j}$). Normalizing the sensitivity coefficients ensures that observed changes are equivalent regardless of the magnitude of the parameter or the state variable. Results of the sensitivity analysis for chemical thyroid concentration and changes in T_3 and T_4 are shown below (Figs. 2A–C).

Exposure level estimations and MOE

Environmental concentrations were found in literature for TCS, BP2, MBT, and RSC. For TCS, reported environmental concentrations ranged from 0.01 mg/kg/d (Allmyr *et al.*, 2009) to 0.08 mg/kg/d (Queckenberg *et al.*, 2010). For BP2, concentrations were found ranging from 0.0016 to 0.00492 mg/kg/d in food, water, and packaging (IARC, 2012). For MBT, concentrations were found ranging from $3.3e^{-4}$ to 0.00418 mg/kg/d in metal working agents or preservatives (USEPA, 1994). For RSC, concentrations were estimated to range from 0.1 to 0.8 mg/kg/d in those who consumed shrimp (EFSA, 2010).

In addition to literature-reported estimates, HT *in silico* models were used to predict distributions of exposure levels. As both maternal and fetal effects of thyroid hormone-perturbing chemicals are often of concern (Gilbert *et al.*, 2012), our analysis focused on females of reproductive age. Exposure level estimates (mg/kg/d) at the 50th and 95th percentiles for the 4 environmental chemicals (MBT, RSC, BP2, and TCS) for females of reproductive age were predicted using the mechanistic High-Throughput Stochastic Human Exposure and Dose Simulation (SHEDS-HT) model (Isaacs *et al.*, 2014). SHEDS-HT was used to simulate exposures for 100 000 simulated individuals to the environmental chemicals based on reported weight fractions (Goldsmith *et al.*, 2014) and population use patterns (Isaacs *et al.*, 2014) for approximately 200 consumer product types. SHEDS-HT estimated exposure levels via dermal, inhalation, and oral routes, and the oral route included both ingestion and transfer of chemical from the hands to the mouth. Dermal removal processes, as well as absorption fractions for the dermal and inhalation routes were applied as described in Isaacs *et al.* (2014). Absorption fractions for the oral route were not modeled in SHEDS-HT; rather, the chemical-specific absorption fractions were obtained from Gastroplus after a 24-h simulation with SHEDS-HT oral intake estimates. Total absorbed dose (in mg/kg/d) was then calculated as the sum of the absorbed doses from all routes. Because SHEDS-HT model was designed for prioritizing chemicals in consumer products, it cannot be used to predict exposure levels for the 2 drugs, PTU and MMI. Thus, population medians (mg/kg/d) of PTU and MMI for females of reproductive age were obtained from a published study that predicted distributions of human exposure levels of 7968 chemicals using a HT, heuristic model with 5 descriptors, including 4 use categories (Wambaugh *et al.*, 2014).

The MOE for each chemical was calculated as the ratio of the ED_{10} and the estimated exposure levels obtained from either literature or the HT exposure models. MOEs were then used to calculate the 'distance' between estimated exposure levels and oral equivalent doses likely to inhibit T_3 or T_4 levels by 10% due to TPO inhibition (the ED_{10}). To estimate the ED_{10}, physiological parameters in the PBPK model were set specifically for females of reproductive age with a BW of 70 kg (Table 3), and thyroid

TABLE 3. Physiological Parameters Used for the Human PBPK Model

Parameter	Value	Source
BW(g)- assume 1 g = 1 ml	70000.0	Brown et al. (1997)
Cardiac Output (Q_CO; ml/min)	5200.0	Brown et al. (1997)
Tissue Volume (as a Fraction of BW)		
Kidney (V_Kid)	0.0040	Brown et al. (1997)
Liver (V_Liv)	0.026	Brown et al. (1997)
GI tract (V_GI)	0.0171	Brown et al. (1997)
Rest of body (V_Rap)	0.0493	Brown et al. (1997); remaining tissues
Muscle (V_Mus)- for females	0.290	Brown et al. (1997)
Skin (V_Skin)- for females	0.031	Brown et al. (1997)
Slowly perfused tissues (V_Slow)- for bone	0.049	Brown et al. (1997)
Adipose (V_Fat)- for females	0.327	Brown et al. (1997)
Brain (V_Brn)	0.020	Brown et al. (1997)
Thyroid (V_Thy)	0.0003	Brown et al. (1997)
Blood (V_Bld)	0.0714	Brown et al. (1997)
Blood Flow (as a Fraction of Cardiac Output)		
Kidney (Q_Kid)	0.175	Brown et al. (1997)
Liver (Q_Liv)	0.227	Brown et al. (1997)
Rest of body (Q_Rap)	Difference	Q_CO—blood flow of all other tissues
Muscle (Q_Mus)	0.191	Brown et al. (1997)
Skin (Q_Skin)	0.058	Brown et al. (1997)
Slowly perfused tissues (Q_Slow)- for bone	0.042	Brown et al. (1997)
Adipose (Q_Fat)	0.085	Brown et al. (1997)
Brain (Q_Brn)	0.114	Brown et al. (1997)
Thyroid (Q_Thy)	0.016	Brown et al. (1997)
Portal vein (Q_PV)	0.181	Brown et al. (1997)
Hepatic artery (Q_HA)	Difference	Q_Liv - Q_PV

hormone parameters in the PD model were set for individuals with normal thyroid hormone concentrations (Table 1).

RESULTS

Total Clearance of Chemicals

Total clearance values for MMI, PTU, and TCS in rats (needed for model evaluation), and total clearance values for all 6 chemicals in humans, are presented in Tables 4 and 5. TCS clearance in rats (4.38 ml/min) was about 10 times greater than the clearance for MMI (0.503 ml/min) and PTU (0.345 ml/min). PTU was estimated to have the largest clearance rate in humans (270 ml/min), followed by RSC (138.8 ml/min) and MMI (80.85 ml/min). The clearance rates for TCS (48.3 ml/min) and MBT (25.5 ml/min) were moderate, and BP2 had the slowest clearance rate of the 6 chemicals (15.8 ml/min) in humans.

Although PK data are readily available for drugs such as PTU and MMI, it is often lacking for environmental chemicals. A review of literature and technical documents failed to reveal information pertaining to human $t_{1/2}$, V_d, or clearance values for BP2, MBT, and RSC. In a prior unpublished analysis not related to this study, measured $t_{1/2}$ values of 670 chemicals were compared against Sarver-predicted values (Equation 3), and the Sarver equation was most appropriate between log *P* values of −4 and 4 (70% within a factor of 5). The log P values of BP2 and MBT were approximately 2.3, while the log *P* value of RCS was approxiamately 1. Although an ideal scenario remains the use of known clearance measurements for chemicals of interest when available, these Sarver-predicted half-lives were within 2-fold difference from those values measured in rats (Garcia, 2004; Jeon *et al.*, 2008; Merker *et al.*, 1982).

Model Evaluation in Rats

For both PTU and MMI, the thyroid lumen-to-blood PC required adjustment from a value similar to kidney-to-blood PC to a value above unity (Table 4) in order to fit data (Cooper *et al.*, 1983, 1984b) that showed higher concentrations in the rat thyroid gland than in blood (Figs. 3a and 4a). These 2 drugs exhibit a longer residence time in the thyroid gland than in blood (Marchant *et al.*, 1972). Both drugs were shown to leave the blood immediately after dosing in the rat model, and this behavior agrees with measured data (Figs. 3b and 4b). In contrast, measured data suggest that both chemicals remain in the thyroid compartment for a longer period of time compared with model simulations (Figs. 3a and 4a). Both MMI and PTU are drugs likely to remain in the thyroid for a duration sufficient to exert their therapeutic effects (Cooper, 2005). This persistence is possibly due to binding or other mechanisms not described in the present model, in which the thyroid gland represents a generic perfusion-limited compartment (Skellern *et al.*, 1980; Wartofsky and Ingbar, 1971) that is generalizable for a wide variety of chemicals rather than for MMI or PTU specifically.

Both PTU and MMI were predicted to reach peak blood concentrations 65 h after dosing, peak thyroid concentrations 70 h after dosing, and then to remain steady until stopping dosage after 7 days. These peak concentrations were 27.2 μg/ml for serum PTU and 0.751 μg/tissue for thyroid PTU, and were 17.3 μg/ml for serum MMI and 0.606 μg/tissue for thyroid MMI. The measured peak concentration of PTU in blood (26.65 μg/ml) was observed immediately after stoppage of the daily 7-day doses (Fig. 3b), while the peak measured concentration in the thyroid gland (0.77 μg/tissue) was observed 17 h after stopping dosage (Fig. 3a). There was a 2 and 26% difference between measured and predicted concentrations of PTU in the blood and thyroid gland, respectively, at the first measured time point. For MMI, the first measured time point occurred 0.6 h after stoppage of the daily 7-day doses, and at this time, concentrations were at their peak in the blood (12.9 μg/ml; Fig. 4b) and in the thyroid gland (0.376 μg/tissue; Fig. 4a). At this time point, predicted blood concentrations had dropped to 11.91 μg/ml, resulting in a percent difference between predicted and measured values of 8%. The percent difference between measured and predicted thyroid concentrations at this time point was 41.1%.

At the end of the 7-day simulated dosing with PTU (on days 6 and 7), predicted levels of both T_3 (Fig. 3c) and T_4 (Fig. 3d) were at their minimum. Two days after the final dosing, both hormones rose above their baseline levels, and both hormones reached their maximum levels approximately 2 weeks after stopping dosage. Seven weeks after stopping dosage, all hormones had returned to their baseline levels. Hormonal changes induced by simulated MMI exposure also resulted in similar trends, though it only required 6 weeks to return to baseline levels (data not shown). Although the PBPK model predicted a more rapid disappearance of MMI and PTU from the thyroid compartment, the accompanying PD model was able to predict hormone concentrations in blood that agreed with measured T_3 (Fig. 3c) and T_4 (Fig. 3d) data observed in recovering rats after dosing with PTU for 7 days (Cooper *et al.*, 1983).

Predicted blood concentrations of TSC in rats reached their peak (454 ng/ml) just 24 min after dosing and then began to decline (Fig. 5). Measured serum concentrations of TCS reached

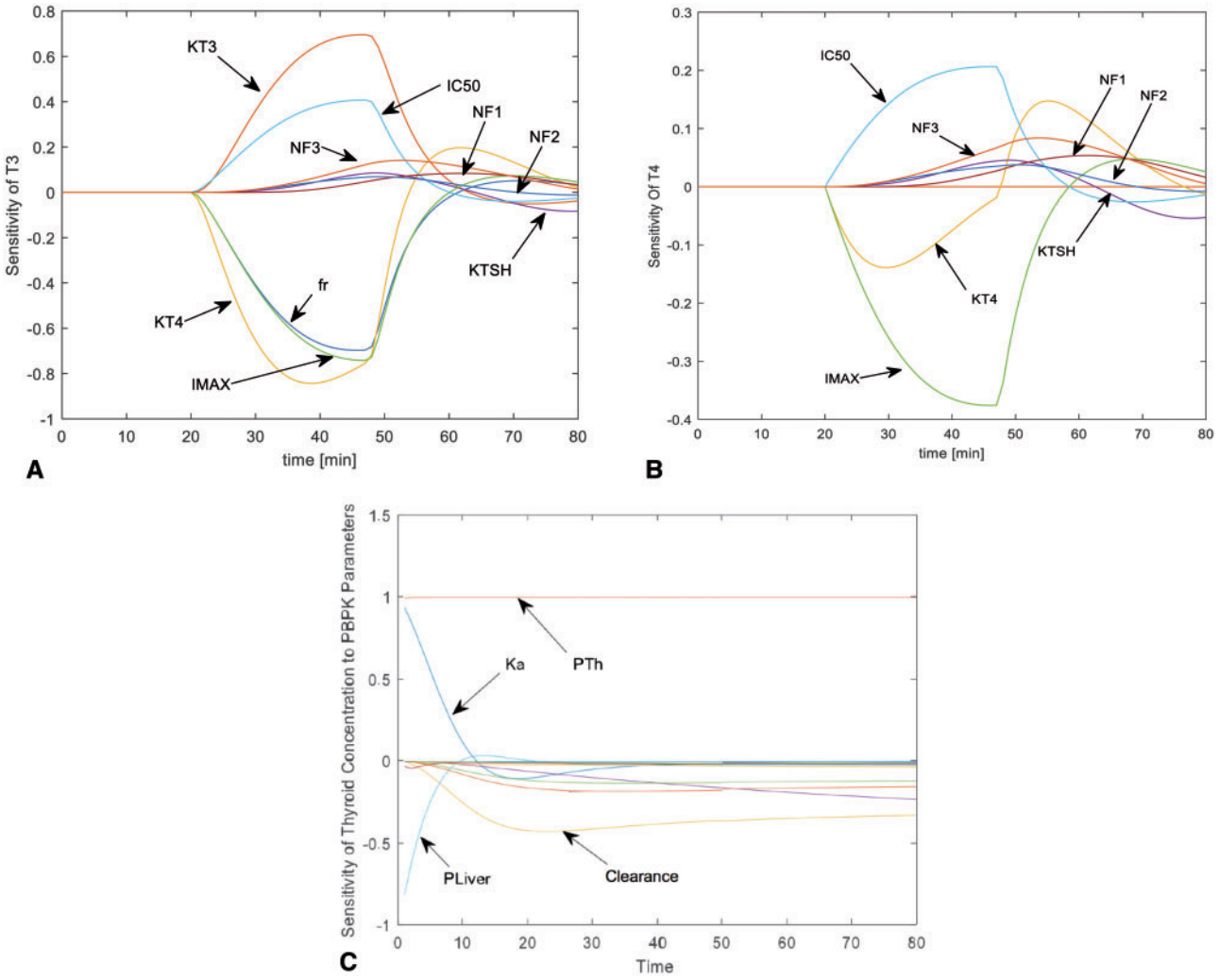

FIG. 2. Results of the sensitivity analysis of physiological parameters influencing changes in T_3 **(A)** and T_4 **(B)** during evaluation of the PD model and chemical concentration in the thyroid gland compartment during evaluation of the PBPK model **(C)**. Abbreviations are as follows: PTh, thyroid lumen-to-plasma PC; PLiv, liver-to-plasma PC; Ka, absorption rate; KT_4, elimination rate of T_4, KTSH, elimination rate of TSH, KT_3, elimination rate of T_3; fr, fraction of T_4 peripherally converted to T_3; NF1-NF3, slope factor constants 1–3 used in the PD model. Unlabeled lines in (C) represent influence of partition coefficients of remaining tissues.

their peak 4 h after dosing. The predicted blood TCS concentration was 5 times higher than the measured concentration at the first measured time point of 43 min (421 vs 81 ng/ml). All other predicted values fell within a 2-fold difference of measured data and appeared to have no systematic errors. All predicted hormonal concentrations at this single oral dosage changed <1% (data not shown). The overall agreement between predicted and measured TCS concentrations suggests that the estimated clearance for TCS is reasonable.

Predicted levels of T_4 were consistent with results observed by Zorrilla *et al.* (2009) and Paul *et al.* (2010) at lower doses (Figs. 6a and c). Predicted levels of T_4, however, were higher than measured values at doses above 30 mg/kg/d. These discrepancies were 2–3 times greater than measured levels for Wistrar rats (Fig. 6a), and were 1.5 times greater than measured data for Long-Evans rats (Fig. 6c). As expected, the smaller decrease in predicted T_4 levels seen at higher doses likely reflects influence from only TPO inhibition in our model, whereas the more pronounced decline in measured data is due to thyroid disruption in general. For example, TCS is thought to result in increased metabolism (eg, sulfation and glucuronidation) of thyroid hormones (Paul *et al.*, 2010). In contrast, there was little difference between predicted and measured levels of T_3 (Figs. 6b and d).

Model Evaluation in Humans

The modified thyroid lumen-to-blood PCs in rats were used in the human model when simulating exposures to MMI and PTU (Table 5). Predicted and measured serum concentrations of MMI after a single oral 30 or 60 mg dose in humans both reached their peaks 2 h after dosing and then declined (Figs. 7a and b). At this time, predicted and measured MMI concentrations at the 30 mg dose were nearly identical (0.60 and 0.651 μg/ml, respectively), while the predicted value at the 60 mg dose (0.773 μg/ml) was 1.29 times less than the measured value (1.20 μg/ml). At both doses, all predicted values fell within a 2-fold difference of measured values and tended to overpredict for 44% of the 9 time points at the 30 mg dose and for 67% of the time points at the 60 mg dose. Hormones returned to their baseline levels 52 days after dosing, after surpassing these levels 21 days after dosing (data not shown). Based upon the agreement between predicted and measured serum concentrations in humans and

TABLE 4. Chemical-Specific Parameters for the Rat PBPK Model

Parameter	Chemical[a]			Source
	MMI	PTU	TCS	
IC_{50} (μM)	0.025	0.12	142	Measured, Paul et al. (2014)
I_{Max} (% activity)	0.9084	0.9426	0.511	Measured, Paul et al. (2014)
Clearance (ml/min)	0.5025	0.345	4.38	Measured, See text
Absorption rate constant (k_a; (1/min)	0.0252	0.018	0.0288	Predicted, GastroPlus
Tissue to Plasma PCs				
Kidney (P_Kid)	0.81	0.41	7.48	Predicted, GastroPlus
Liver (P_Liv)	0.75	0.36	8.20	Predicted, GastroPlus
Rest of body (P_Rap)- for lung	0.82	0.48	9.39	Predicted, GastroPlus
Muscle (P_Mus)	0.77	0.33	4.55	Predicted, GastroPlus
Skin (P_Skin)	0.69	0.48	10.56	Predicted, GastroPlus
Yellow marrow (P_Slow)	0.16	0.20	59.61	Predicted, GastroPlus
Adipose (P_Fat)	0.16	0.20	59.61	Predicted, GastroPlus
Brain (P_Brain)	0.87	0.45	19.70	Predicted, GastroPlus
Thyroid (P_Thyroid)	2.80	2.21	7.48	Predicted, GastroPlus or fitted[b]

[a]Chemical abbreviations: MMI, methimazole; PTU, 6-propylthiouracil; TCS, triclosan.
[b]The thyroid to plasma PC for TCS was set to that of kidney to plasma PC with the observation that these values are similar (Merrill et al. 2005). For MMI and PTU, this value was fitted in order to simulate the higher concentration of chemical in tissue compared with plasma, as shown by measured data.

TABLE 5. Chemical-Specific Parameters for the Human PBPK Model

Parameter	Chemical[a]						Source
	MMI	PTU	BP2	MBT	TCS	RSC	
IC_{50} (μM)	0.025	0.12	0.16	0.45	142	253	Measured, Paul et al. (2014)
I_{Max} (% activity)	0.9084	0.9426	0.9059	0.9684	0.511	0.229	Measured, Paul et al. (2014)
Clearance (ml/min)	80.9	270.0	15.8	25.5	48.3	139.1	Measured and predicted[b]
Absorption rate constant (k_a; 1/min)	0.0087	0.0078	0.009	0.012	0.0438	0.0096	Predicted, GastroPlus
Tissue to Plasma PCs							
Kidney (P_Kid)	0.81	0.42	0.20	0.88	3.98	0.82	Predicted, GastroPlus
Liver (P_Liv)	0.80	0.42	0.18	1.28	6.55	0.88	Predicted, GastroPlus
Rest of body (P_Rap)- for lung	0.82	0.43	0.23	0.41	0.91	0.76	Predicted, GastroPlus
Muscle (P_Mus)	0.78	0.36	0.13	0.83	4.02	0.79	Predicted, GastroPlus
Skin (P_Skin)	0.75	0.51	0.35	1.14	4.99	0.81	Predicted, GastroPlus
Yellow marrow (P_Slow)	0.21	0.21	0.18	1.79	23.85	0.37	Predicted, GastroPlus
Adipose (P_Fat)	0.21	0.21	0.18	1.79	23.85	0.37	Predicted, GastroPlus
Brain (P_Brain)	0.87	0.47	0.20	1.92	10.48	1.03	Predicted, GastroPlus
Thyroid (P_Thyroid)	2.80	2.21	0.20	0.88	3.98	0.82	Predicted, GastroPlus or fitted[c]

[a]Chemical abbreviations: MMI, methimazole; PTU, 6-propylthiouracil; BP2, benzophenone-2; MBT, 2-mercatobenzothiazole; TCS, triclosan; RSC, resorcinol.
[b]Total clearance was taken for each chemical as a function of $t_{1/2}$ and V_d. Clearance for MMI, PTU, and TCS used measured values for $t_{1/2}$ and V_d. Clearance for BP2, RSC, and MBT used predicted V_d from ADMET Predictor software and $t_{1/2}$ predicted using the equation from Sarver et al. (1997). See text for additional details.
[c]The thyroid to plasma PC was set to that of kidney to plasma PC with the observation that these values are similar (Merrill et al., 2005). For MMI and PTU, this value was adjusted to that in the rat used to fit measured data showing higher concentrations of the drugs in the thyroid compared with within blood.

rats, as well as thyroid hormone levels in rats, the combined PBPK/PD model is appropriate for estimating oral doses of chemicals that can lead to thyroid concentrations capable of inhibiting TPO.

MOE for TPO Inhibitors

The IC_{50} values obtained from the HT *in vitro* study for the 6 selected chemicals ranged from 0.025 to 253 μmol/l, while I_{Max} ranged from 23 to 97% inhibition (Table 5). Despite the high potencies of MMI and PTU, their exposure estimates are negligible at the HT *in silico* model predicted median, leading to MOE estimates above 1000 (Table 6). The predicted exposure levels for MBT were the lowest among the 4 environmental chemicals, but MBT was of medium concern at the 95th percentile exposure level due to its estimated clearance rate, which was second lowest among the 6 chemicals. Literature-reported environmental concentrations of MBT (USEPA, 1994), however, were at least 2 orders of magnitude greater than the predicted distribution of exposure levels, leading to MOE estimates <50 (Tables 6 and 7) and suggesting that MBT is of greater concern than indicated using predicted exposure levels.

Model-predicted exposure levels for BP2, RSC, and TCS at the 95th percentile ranged from 0.01 to 0.1 mg/kg/d, or about 5 orders of magnitude greater than those of the other 3 chemicals (Table 7). TCS was also the only chemical that had an appreciable exposure level predicted at the 50th percentile (0.02 mg/kg/d). Thus, despite its low potency, the high predicted exposure levels of TCS resulted in a MOE of approximately 200 at the predicted population exposure level at the 50th percentile (Table 6)

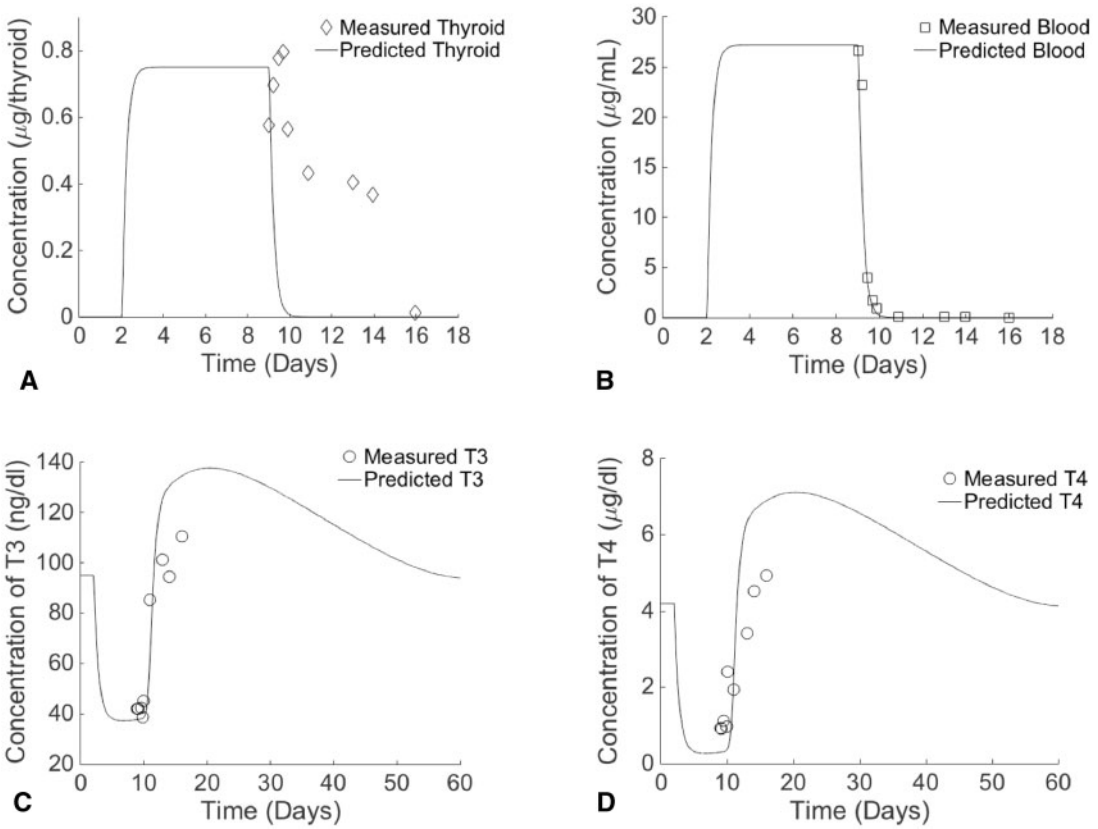

FIG. 3. Time-course measured and predicted concentrations of 6-PTU in the thyroid gland tissue **(A)** and blood **(B)** of rats provided 0.05% PTU in drinking water for 7 days and PTU-induced changes in predicted and measured rat T_3 **(C)** and T_4 **(D)** serum concentrations. Measured data taken from Cooper *et al.* (1983).

and a MOE below 50 at the 95th percentile (Table 7). In addition, the MOE for TCS remained below 50 at the high end of the literature-reported exposure level (Table 7) and increased to 400 at the low end of the literature-reported exposure level (Table 6).

Both the high predicted exposure level at the 95th percentile and slow clearance rate of BP2 resulted in it having a MOE below 10, which is similar to that using literature-reported exposure levels (Table 7). The predicted exposure level at the 50th percentile, however, is much lower than literature-reported values, making the MOE at this predicted exposure level highly uncertain (Table 6). For RSC, predicted exposure levels at both 50th and 95th percentiles were much lower than literature-reported values. MOE estimates fall from above 1000 using predicted exposure levels to below 1000 at the lowest literature-reported concentration (Table 6) and below 100 at the highest literature-reported concentration (Table 7). This finding suggests that RSC also might be of greater concern than indicated using predicted exposure levels.

DISCUSSION

In humans, thyroid binding globulin is abundant and has a high affinity for thyroid hormones, while this serum protein is absent in rats (Oppenheimer, 1968; Refetoff, 1970). This species difference should be considered when thyroid hormone kinetics and diffusion to tissues are investigated. However, in our analyses, total hormone levels, including both free and bound, in blood were the endpoints of interest. Therefore, differences in binding between species should not affect the predictions of hormone levels, or subsequently, the estimates of MOEs. In addition, the agreement observed between measured and predicted blood concentrations of PTU, MMI, and TCS in rats, and of MMI in humans, also suggests that exclusion of species-dependent plasma protein binding mechanisms in our PBPK model is nonproblematic.

The 2 most potent (ie, lowest IC_{50} values) chemicals within this study, MMI and PTU, are drugs used to treat mild to severe thyrotoxicosis (Carroll and Matfin, 2010). Within the thyroid compartment itself, MMI is generally irreversibly bound to the TPO enzyme (Cooper, 2005). In contrast, PTU exerts its efficacy through its structural similarity to the iodide substrate and so easily and reversibly binds to the TPO enzyme. There are likely additional mechanisms at work that are influencing the accumulation of these 2 drugs in the thyroid gland, such as the influence of the sodium/iodide basolateral symporter protein (Pesce and Kopp, 2014). Without data, however, to support the incorporation of these other mechanisms into our PBPK model, a simpler adjustment of the thyroid lumen-to-blood PC was a reasonable approach to simulate the disposition of these 2 drugs. In MOE estimation for MMI and PTU, their high potencies were countered by low exposure level predictions (Wambaugh *et al.*, 2014). It is reasonable to assume that exposure to these 2 drugs occurs primarily to individuals taking the medications and that little enters into the environment. Therefore, even with the uncertainties in estimating thyroid concentrations of these 2 drugs, there is low concern of TPO inhibition from exposures to these 2 drugs in the environment.

TCS was originally used as a negative control in the HT *in vitro* study (Paul *et al.*, 2014) because of previously reported negative TPO activity (Crofton *et al.*, 2007; Paul *et al.*, 2013). In contrast, Paul *et al.* (2014) concluded that TCS may inhibit TPO weakly, evident with the enhanced sensitivity of the Amplex

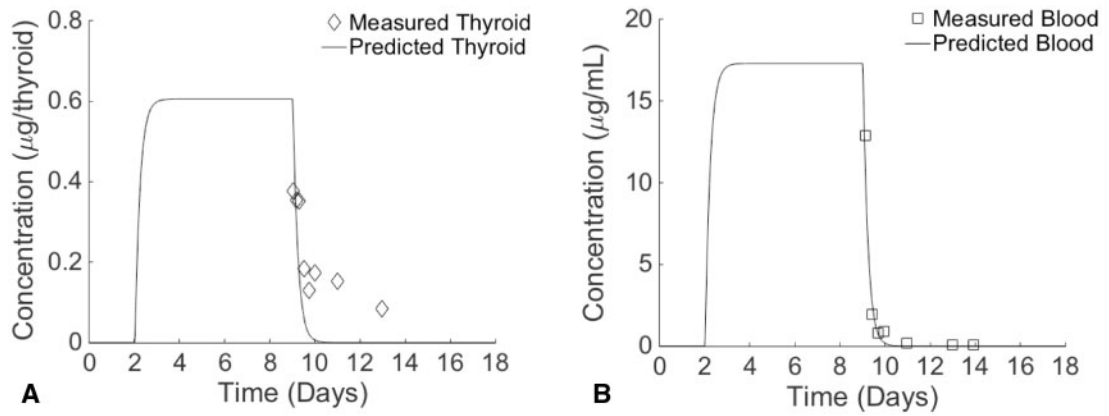

FIG. 4. Time-course measured and predicted concentrations of MMI in the thyroid gland tissue **(A)** and blood **(B)** of rats provided 0.05% MMI in drinking water for 7 days. Measured data taken from Cooper *et al.* (1984b).

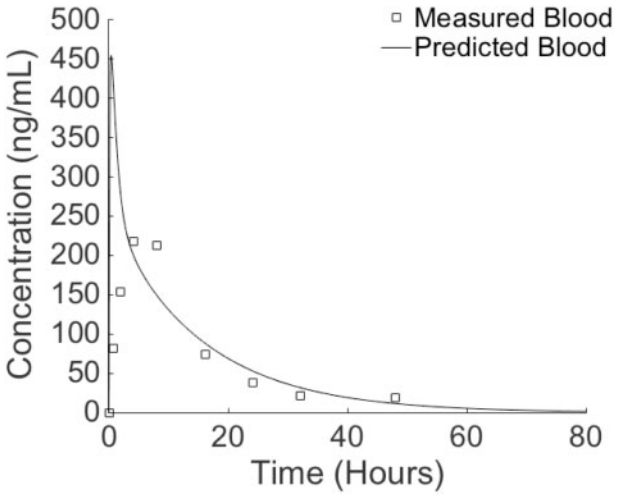

FIG. 5. Time-course measured and predicted concentrations of TCS in the blood of rats provided a single oral dose of 5 mg/kg in 1 ml corn oil. Measured data taken from Wu *et al.* (2009).

UltraRed-based assay. Although it can be debated whether TCS does in fact inhibit the TPO enzyme, this chemical's thyroid-disrupting properties cannot be argued (Crofton *et al.*, 2007; Paul *et al.*, 2010; Stoker *et al.*, 2010). Due to its high exposure potential (Thompson *et al.*, 2005), TCS appears to be of high concern based on its MOE, even though its very low potency leads to the second lowest ED_{10} among the 6 selected chemicals. This result by no means suggests that TCS should be prioritized as a TPO inhibitor. However, given the knowledge of TCS as a thyroid-disrupting chemical in general and its abundance in consumer products, further studies may be warranted in order to ascertain its TPO-inhibiting potential.

The uncertainty associated with the estimated MOE values is inversely proportional to estimated exposure concentrations and directly proportional to the ED_{10}. The large discrepancies between literature-reported and model-predicted exposure levels and resultant MOE estimates for the 4 environmental chemicals illustrate the large uncertainty inherent in both the heuristics-based model (Wambaugh *et al.*, 2014) and the SHEDS-HT. These models were developed for exposure-based prioritization of chemicals, and thus, by design these models take limited amounts of data (eg, chemical or product use descriptors) to rapidly produce exposure estimates with large margins of error. For example, SHEDS-HT was designed to be conservative with respect to several model parameters, such as the number of product types in which chemicals are found, chemical concentrations in various formulations, and differential consumer product use patterns. However, even with large uncertainties, these models can provide useful metrics for discriminating among chemicals when environmental data are lacking. The MOE values presented here do not represent a rank-ordering of risk *per se*, but rather should be used to separate chemicals into bins of low, medium, and high concerns. For example, a MOE of 1000 or 10 000 will both be considered as low concern; while a MOE of 2 or 100 will both be considered as high concern. Improving these HT exposure models and reducing the uncertainty in their predictions to support the development of risk-based metrics is an area of ongoing research. Results from published studies often reflect exposure to those groups most highly exposed (eg, pesticide applicators), which can further explain the large differences between predicted and literature-reported exposure values. It should be noted that measured exposure levels also hold a certain degree of uncertainty due to the difficulty in measuring external exposure concentrations from all sources (eg, food, water, product use). Such uncertainty in exposure concentration is likely more challenging to characterize than the uncertainty associated with PK and PD parameters.

The other source of uncertainty in MOE calculations lies in the estimate of clearance rates, as the ED_{10} is partly a function of the clearance rate. The clearance rates for MMI, PTU, and TCS were determined using literature-reported half-lives, so these estimates should be reasonably accurate. Using the half-lives of BP2, MBT, and RSC estimated in rats (Garcia, 2004; Jeon *et al.*, 2008; Merker *et al.*, 1982) to compare with the use of half-lives predicted from the Sarver equation (Equation 3), it was found that MOE estimates are much more robust to uncertainty in clearance, compared with uncertainty in exposure estimates. For example, replacing the Sarver-predicted $t_{1/2}$ value with the rat value (Jeon *et al.*, 2008) for BP2 resulted in a slight decrease in clearance rate from 15 to 10 ml/min, and the MOE estimate continues to indicate high concern (below 10). The rat $t_{1/2}$ of MBT (Garcia, 2004) is approximately 2 times lower than the Sarver-predicted value, and predicted estimates of clearance are more conservative (25 vs 60 ml/min). Despite this difference, the MOE estimate for MBT remains above 1000 and continues to indicate

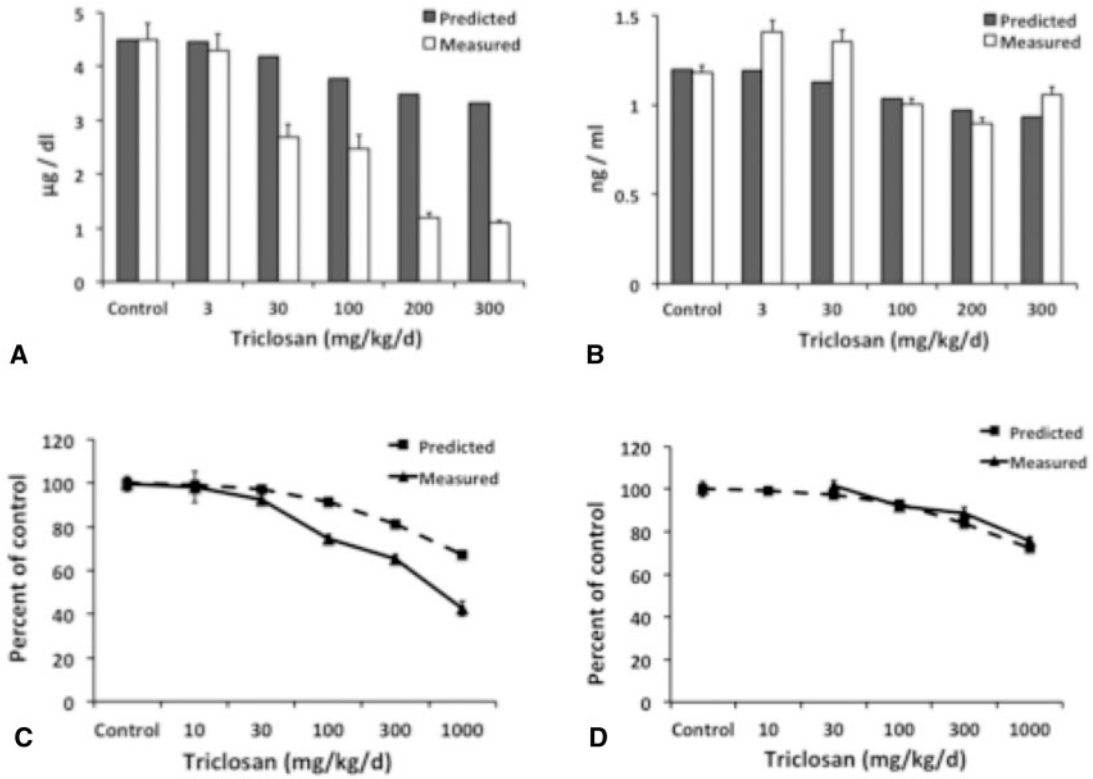

FIG. 6. Measured and predicted changes in T_4 **(A)** and T_3 **(B)** levels in the serum of male Wistrar rats after 31 days of dosing, and percent change from the control for T_4 **(C)** and T_3 **(D)** in the serum of female Long-Evans rats after 4 days of dosing. Measured data taken from Zorrilla *et al.* (2009) and Paul *et al.* (2010). Error bars of measured data represent SE.

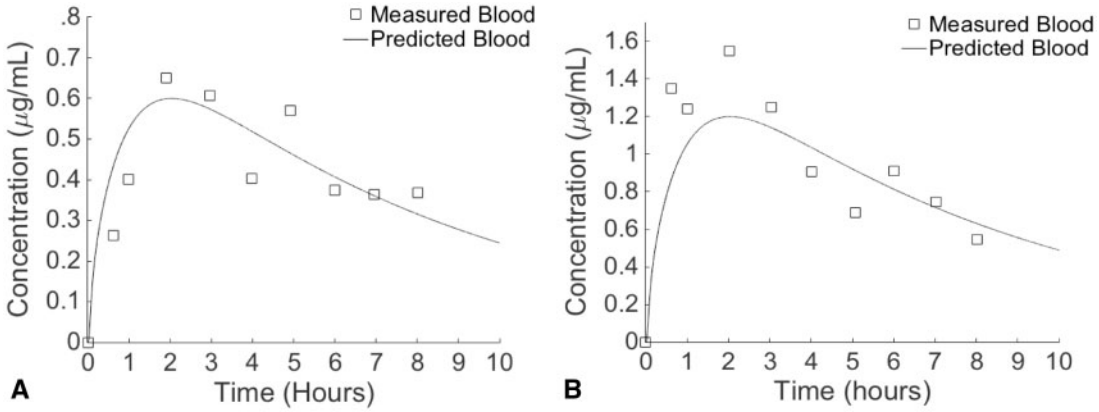

FIG. 7. Time-course measured and predicted concentrations of MMI in the blood of humans provided a single oral dose of 30 mg **(A)** or 60 mg **(B)**. Measured data taken from Cooper *et al.* (1984a).

low concern. In contrast to MBT, the rat $t_{1/2}$ of RSC (Merker *et al.*, 1982) is approximately 2 times lower than the Sarver-predicted value, and predicted estimates are less conservative (139 vs 65 ml/min). RSC continues to exhibit the highest clearance rate among the selected chemicals, despite this apparent fall in rate, and the MOE estimates continue to remain very high (>5000), indicating the very low concern for this chemical.

Coupling HT *in vitro* toxicity data with appropriately parameterized computational models that quantitatively link exposure to internal tissue dose-response can generate regulatory-relevant predictions of biological responses and adverse outcomes for reducing uncertainties in risk assessment. When multiple computational models are used in concert to derive values that allow comparisons among chemicals, such as MOE estimates, confidence in the results is limited by the weakest model in the series. When chemical-specific data on exposure levels and ADME characteristics are available, more reliable MOE estimates may be achieved. Such an approach is limited; however, when data for calibrating or evaluating predictive models is missing or when high degrees of uncertainties are present in toxicity data or exposure/dosimetry predictions. Although the framework presented in this study may be used as a screening tool to prioritize chemicals in a HT manner, our recommendation is to use this MOE approach primarily when some chemical-specific data is available to evaluate predictions of exposure potentials, hazard potentials, and ADME behaviors. Incorporating the

TABLE 6. MOE Based on the Target-Tissue Concentrations of TPO Inhibiting Compounds[a] Expected to Result in a 10% Decline in Circulating T_4 and T_3 Levels Compared with Predicted Environmental Exposures at the 50th Percentile of the Population and Low End Literature-Reported Values

Chemical	IC_{50}	T_3 ED_{10} (mg/kg/d)	50th percentile (mg/kg/d)	MOE	Measured (mg/kg/d)[b]	MOE
TCS	142	4.19	1.98E-02	211	1.00E-02	419
MMI	0.025	2.86E-04	4.18E-08	6840	N/A	Not calculated
PTU	0.12	1.38E-02	1.31E-07	105,000	N/A	Not calculated
RSC	253	130	2.60E-06	50 000 000	1.00E-01	1300
BP2	0.16	1.09E-02	Below detection	Not calculated	1.60E-03	7
MBT	0.45	7.06E-03	Below detection	Not calculated	3.30E-04	21
Chemical	**IC_{50}**	**T_4 ED_{10} (mg/kg/d)**	**50th percentile (mg/kg/d)**	**MOE**	**Measured (mg/kg/d)[b]**	**MOE**
TCS	142	4.12	1.98E-02	209	1.00E-02	412
MMI	0.025	2.84E-04	4.18E-08	6790	N/A	Not calculated
PTU	0.12	8.24E-03	1.31E-07	62 900	N/A	Not calculated
RSC	253	128.17	2.60E-06	49 300 000	1.00E-01	1282
BP2	0.16	1.08E-02	Below detection	Not calculated	1.60E-03	7
MBT	0.45	7.01E-03	Below detection	Not calculated	3.30E-04	21

[a]Chemical abbreviations: MMI, methimazole; PTU, 6-propylthiouracil; BP2, benzophenone-2; MBT, 2-mercatobenzothiazole; TCS, triclosan; RSC, resorcinol.
[b]No measured concentrations could be obtained from the literature for MMI and PTU. See text for references for the measured exposure levels of the 4 environmental chemicals.

TABLE 7. MOE Based on the Target-Tissue Concentrations of TPO Inhibiting Compounds[a] Expected to Result in a 10% Decline in Circulating T_4 and T_3 Levels Compared with Predicted Environmental Exposures at the 95th Percentile of the Population and High End Literature-Reported Values

Chemical	IC_{50}	T_3ED_{10} (mg/kg/d)	95th percentile (mg/kg/d)	MOE	Measured (mg/kg/d)	MOE
BP2	0.16	1.09E-02	5.38E-03	2	4.92E-03	2
TCS	142	4.19	9.61E-02	42	8.40E-02	50
MBT	0.45	7.06E-03	4.74E-06	1496	4.18E-03	2
RSC	253	130	1.15E-02	11 607	8.00E-01	163
Chemical	**IC_{50}**	**T_4ED_{10} (mg/kg/d)**	**95th percentile (mg/kg/d)**	**MOE**	**Measured (mg/kg/d)**	**MOE**
BP2	0.16	1.08E-02	5.38E-03	2	4.92E-03	2
TCS	142	4.12	9.61E-02	42	8.40E-02	49
MBT	0.45	7.01E-03	4.74E-06	1485	4.18E-03	2
RSC	253	128.17	1.15E-02	11 443	8.00E-01	160

[a]Chemical abbreviations: BP2, benzophenone-2; MBT, 2-mercatobenzothiazole; TCS, triclosan; RSC, resorcinol. No predictions at this percentile were available for the 2 drugs MMI or 6-PTU.
[b]No measured concentrations could be obtained from the literature for MMI and PTU, and predictions were not available at the 95th percentile for these 2 drugs. See text for references for the measured exposure levels of the 4 environmental chemicals.

relationship between environmental exposure and target tissue dose, through consideration of related ADME properties and within the context of the biological events described by the AOP of concern, offers the potential for reducing uncertainty in chemical prioritization and risk assessment.

CONCLUSIONS

This study utilizes known biological and chemical-specific information to design and implement a combined PBPK/PD model to examine a chemical's potential for TPO inhibition. Such an effort will aid decision makers in their prioritization of chemicals screened in a higher throughput manner. Integration of hazard data from HT *in vitro* tests, HT exposure predictions or literature-reported levels, and ADME-related considerations can aid in the screening of chemicals of concern, as demonstrated from this study using chemicals with varying degrees of TPO inhibiting activity, exposure levels, and ADME properties. There is clear evidence that simply assessing the health risk of a chemical by its potency, as determined solely through *in vitro* testing, may be misleading and that both exposure and consideration of ADME-related properties to determine internal dosimetry would reduce uncertainty and increase confidence in the chemical screening process.

SUPPLEMENTARY DATA

Supplementary data are available online at http://toxsci.oxfordjournals.org/.

Disclaimer

This article has been reviewed in accordance with the policy of the National Health and Environmental Effects Research Laboratory, U.S. Environmental Protection Agency, and approved for publication. Approval does not signify that the contents necessarily reflect the views and policies of the Agency, nor does mention of trade names or commercial products constitute endorsement or recommendation for use.

FUNDING

Jeremy Leonard was funded through the Oak Ridge Institute for Science and Education Research Participation Program at the U.S. EPA.

REFERENCES

Allmyr, M., Panagiotidis, G., Sparve, E., Diczfalusy, U., and Sandborgh-Englund, G. (2009). Human exposure to triclosan via toothpaste does not change CYP3a4 activity or plasma concentrations of thyroid hormones. *Basic Clin. Pharmacol. Toxicol.* **105**, 339–344.

Ankley, G. T., Bennett, R. S., Erickson, R. J., Hoff, D. J., Hornung, M. W., Johnson, R. D., Mount, D. R., Nichols, J. W., Russom, C. L., Schmieder, P. K., *et al.* (2010). Adverse outcome pathways: A conceptual framework to support ecotoxicology research and risk assessment. *Environ. Toxicol. Chem. SETAC* **29**, 730–741.

Brown, R. P., Delp, M. D., Lindstedt, S. L., Rhomberg, L. R., and Beliles, R. P. (1997). Physiological parameter values for physiologically based pharmacokinetic models. *Toxicol. Ind. Health* **13**, 407–484.

Carroll, R., and Matfin, G. (2010). Endocrine and metabolic emergencies: thyroid storm. *Ther. Adv. Endocrinol. Metab.* **1**, 139–145.

Choksi, N. Y., Jahnke, G. D., St Hilaire, C., and Shelby, M. (2003). Role of thyroid hormones in human and laboratory animal reproductive health. *Birth Defects Res. B Dev. Reprod. Toxicol.* **68**, 479–491.

Cooper, D. S. (2005). Antithyroid Drugs. *N. Engl. J. Med* **352**, 905–917.

Cooper, D. S., Bode, H. H., Nath, B., Saxe, V., Maloof, F., and Ridgway, E. C. (1984a). Methimazole pharmacology in man: studies using a newly developed radioimmunoassay for methimazole. *J. Clin. Endocrinol. Metab* **58**, 473–479.

Cooper, D. S., Kieffer, J. D., Halpern, R., Saxe, V., Mover, H., Maloof, F., and Ridgway, E. C. (1983). Propylthiouracil (PTU) pharmacology in the rat. II. Effects of PTU on thyroid function. *Endocrinology* **113**, 921–928.

Cooper, D. S., Kieffer, J. D., Saxe, V., Mover, H., Maloof, F., and Ridgway, E. C. (1984b). Methimazole pharmacology in the rat: studies using a newly developed radioimmunoassay for methimazole. *Endocrinology* **114**, 786–793.

Crofton, K. M., Craft, E. S., Hedge, J. M., Gennings, C., Simmons, J. E., Carchman, R. A., Carter, W. H., and DeVito, M. J. (2005). Thyroid-Hormone–Disrupting Chemicals: Evidence for dose-dependent additivity or synergism. *Environ. Health Perspect.* **113**, 1549–1554.

Crofton, K. M., Paul, K. B., DeVito, M. J., and Hedge, J. M. (2007). Short-term in vivo exposure to the water contaminant triclosan: Evidence for disruption of thyroxine. *Environ. Toxicol. Pharmacol.* **24**, 194–197.

Edwards, S. W., Tan, Y. M., Villeneuve, D. L., Meek, M. E., and Bette, McQueen, C. A. (2015). Adverse outcome pathways – Organizing toxicological information to improve decision making. *J. Pharmacol. Exp. Ther.* Accessed November 4, 2015. doi:10.1124/jpet.115.228239.

Ekerot, P., Ferguson, D., Glämsta, E. L., Nilsson, L. B., Andersson, H., Rosqvist, S., and Visser, S. A. G. (2013). Systems pharmacology modeling of drug-induced modulation of thyroid hormones in dogs and translation to human. *Pharm. Res.* **30**, 1513–1524.

European Food Safety Authority (EFSA). (2010). Scientific opinion on the use of resorcinol as a food additive. *EFSA J.* **8**, 41.

Garcia, H. (2004). *Spacecraft Water Exposure Guidelines for Selected Contaminants: Volume 1, Appendix 5: 2-Mercaptobenzothiazole*. National Academies Press, Washington, DC. Accessed December 3, 2015.

Gilbert, M. E., Rovet, J., Chen, Z., and Koibuchi, N. (2012). Developmental thyroid hormone disruption: Prevalence, environmental contaminants and neurodevelopmental consequences. *NeuroToxicology* **33**, 842–852.

Giles, H. G., Long, J. P., Orrego, H., and Sellers, E. M. (1982). Mechanism of alterations in propylthiouracil disposition after long-term therapy. *Clin. Pharmacol. Ther.* **31**, 559–563.

Goldsmith, M. R., Grulke, C. M., Brooks, R. D., Transue, T. R., Tan, Y. M., Frame, A., Egeghy, P. P., Edwards, R., Chang, D. T., Tornero-Velez, R., *et al.* (2014). Development of a consumer product ingredient database for chemical exposure screening and prioritization. *Food Chem. Toxicol.* **65**, 269–279.

Groh, K. J., Carvalho, R. N., Chipman, J. K., Denslow, N. D., Halder, M., Murphy, C. A., Roelofs, D., Rolaki, A., Schirmer, K., and Watanabe, K. H. (2015). Development and application of the Adverse Outcome Pathway framework for understanding and predicting chronic toxicity: I. Challenges and research needs in ecotoxicology. *Chemosphere* **120**, 764–777.

Hengstmann, J. H., and Hohn, H. (1985). Pharmacokinetics of methimazole in humans. *Klin. Wochenschr* **63**, 1212–1217.

Huffman, L., and Hedge, G. A. (1986). Neuropeptide control of thyroid blood flow and hormone secretion in the rat. *Life Sci.* **39**, 2143–2150.

International Agency for Research on Cancer (IARC). (2012). *Some Chemicals Present in Industrial and Consumer Products, Food, and Drinking Water: Benzophenone. Volume 101*. Available at: http://monographs.iarc.fr/ENG/Monographs/Vol15101/index.php. Accessed December 3, 2015.

Isaacs, K. K., Glen, W. G., Egeghy, P., Goldsmith, M. R., Smith, L., Vallero, D., Brooks, R., Grulke, C. M., and Özkaynak, H. (2014). SHEDS-HT: an integrated probabilistic exposure model for prioritizing exposures to chemicals with near-field and dietary sources. *Environ. Sci. Technol.* **48**, 12750–12759.

Jameson, J. L., and Wheetman, A. P. (2001). Disorders of the thyroid gland. In *Harrison's Principles of Internal Medicine* (E. Braunwald, A. S. Fauci, D. L. Kasper, S. L. Hauser, D. L. Longo, and J. L. Jameson, Eds.), pp. 2048–2060. McGraw-Hill, New York, NY.

Jeon, H. K., Sarma, S. N., Kim, Y. J., and Ryu, J. C. (2008). Toxicokinetics and metabolism of benzophenone-type UV filters in rats. *Toxicology* **248**, 89–95.

Judson, R. S., Kavlock, R. J., Setzer, R. W., Hubal, E. A. C., Martin, M. T., Knudsen, T. B., Houck, K. A., Thomas, R. S., Wetmore, B. A., and Dix, D. J. (2011). Estimating toxicity-related biological pathway altering doses for high-throughput chemical risk assessment. *Chem. Res. Toxicol.* **24**, 451–462.

Jugan, M. L., Levi, Y., and Blondeau, J. P. (2010). Endocrine disruptors and thyroid hormone physiology. *Biochem. Pharmacol.* **79**, 939–947.

Kampmann, J. P., and Hansen, J. M. (1981). Clinical pharmacokinetics of antithyroid drugs. *Clin. Pharmacokinet.* **6**, 401–428.

Kampmann, J., and Skovsted, L. (1974). The Pharmacokinetics of Propylthiouracil. *Acta Pharmacol. Toxicol. (Copenh.)* **35**, 361–369.

Marchant, B., Alexander, W. D., Lazarus, J. H., Lees, J., and Clark, D. H. (1972). The acclumulation of 35 S-antithyroid drugs by the thyroid gland. *J. Clin. Endocrinol. Metab.* **34**, 847–851.

McGuire, R. A., and Hays, M. T. (1981). A kinetic model of human thyroid hormones and their conversion products. *J. Clin. Endocrinol. Metab.* **53**, 852–862.

Merker, P. C., Yeung, D., Doughty, D., and Nacht, S. (1982). Pharmacokinetics of resorcinol in the rat. *Res. Commun. Chem. Pathol. Pharmacol.* **38**, 367–388.

Merrill, E. A., Clewell, R. A., Robinson, P. J., Jarabek, A. M., Gearhart, J. M., Sterner, T. R., and Fisher, J. W. (2005). PBPK model for radioactive iodide and perchlorate kinetics and perchlorate-induced inhibition of iodide uptake in humans. *Toxicol. Sci.* **8**, 25–43.

Nicoloff, J. T., Low, J. C., Dussault, J. H., and Fisher, D. A. (1972). Simultaneous measurement of thyroxine and triiodothyronine peripheral turnover kinetics in man. *J. Clin. Invest.* **51**, 473–483.

Nong, A., Teeguarden, J. G., Clewell, H. J., Dorman, D. C., and Andersen, M. E. (2008). Pharmacokinetic modeling of manganese in the rat IV: Assessing factors that contribute to brain accumulation during inhalation exposure. *J. Toxicol. Environ. Health Part A* **71**, 413–426.

Odell, W. D., Utiger, R. D., Wilber, J. F., and Condliffe, P. G. (1967). Estimation of the secretion rate of thyrotropin in man. *J. Clin. Invest.* **46**, 953–959.

Oppenheimer, J. H. (1968). Role of plasma proteins in the binding, distribution and metabolism of the thyroid hormones. *N. Engl. J. Med.* **278**, 1153–1162.

Oppenheimer, J. H., Schwartz, H. L., and Surks, M. I. (1972). Propylthiouracil inhibits the conversion of L-thyroxine to L-triiodothyronine. An explanation of the antithyroxine effect of propylthiouracil and evidence supporting the concept that triiodothyronine is the active thyroid hormone. *J. Clin. Invest.* **51**, 2493–2497.

Paul, K. B., Hedge, J. M., DeVito, M. J., and Crofton, K. M. (2010). Short-term exposure to triclosan decreases thyroxine *in vivo* via upregulation of hepatic catabolism in young Long-Evans rats. *Toxicol. Sci.* **113**, 367–379.

Paul, K. B., Hedge, J. M., Macherla, C., Filer, D. L., Burgess, E., Simmons, S. O., Crofton, K. M., and Hornung, M. W. (2013). Cross-species analysis of thyroperoxidase inhibition by xenobiotics demonstrates conservation of response between pig and rat. *Toxicology* **312**, 97–107.

Paul, K. B., Hedge, J. M., Rotroff, D. M., Hornung, M. W., Crofton, K. M., and Simmons, S. O. (2014). Development of a thyroperoxidase inhibition assay for high-throughput screening. *Chem. Res. Toxicol.* **27**, 387–399.

Pesce, L., and Kopp, P. (2014). Iodide transport: implications for health and disease. *Int. J. Pediatr. Endocrinol.* **2014**, 8.

Phillips, M. B., Leonard, J. A., Grulke, C. M., Chang, D., Edwards, S. W., Brooks, R., Goldsmith, M. R., El-Masri, H. A., and Tan, Y. M. (2016). A workflow to investigate exposure and pharmacokinetics influences on high-throughput *in vitro* chemical screening based on Adverse Outcome Pathways. *Environ. Health Perspect.* **124**, 53–60.

Queckenberg, C., Meins, J., Wachall, B., Doroshyenko, O., Tomalik-Scharte, D., Bastian, B., Abdel-Tawab, M., and Fuhr, U. (2010). Absorption, pharmacokinetics, and safety of triclosan after dermal administration. *Antimicrob. Agents Chemother.* **54**, 570–572.

Refetoff, S., Robin, N. I., and Fang, V. S. (1970). Parameters of thyroid function in serum of 16 selected vertebrate species: a study of PBI, serum T4, free T4, and the pattern of T4 and T3 binding to serum proteins. *Endocrinology* **86**, 793–805.

Ridgway, E. C., Weintraub, B. D., and Maloof, F. (1974). Metabolic clearance and production rates of human thyrotropin. *J. Clin. Invest.* **53**, 895–903.

Rodgers, T., Leahy, D., and Rowland, M. (2005). Physiologically based pharmacokinetic modeling 1: Predicting the tissue distribution of moderate-to-strong bases. *J. Pharm. Sci.* **94**, 1259–1276.

Rodgers, T., and Rowland, M. (2006). Physiologically based pharmacokinetic modelling 2: Predicting the tissue distribution of acids, very weak bases, neutrals and zwitterions. *J. Pharm. Sci.* **95**, 1238–1257.

Sandborgh-Englund, G., Adolfsson-Erici, M., Odham, G., and Ekstrand, J. (2006). Pharmacokinetics of triclosan following oral ingestion in humans. *J. Toxicol. Environ. Health A* **69**, 1861–1873.

Sarver, J. G., White, D., Erhardt, P., and Bachmann, K. (1997). Estimating xenobiotic half-lives in humans from rat data: influence of log P. *Environ. Health Perspect.* **105**, 1204–1209.

Silva, J. E., Gordon, M. B., Crantz, F. R., Leonard, J. L., and Larsen, P. R. (1984). Qualitative and quantitative differences in the pathways of extrathyroidal triiodothyronine generation between euthyroid and hypothyroid rats. *J. Clin. Invest.* **73**, 898–907.

Sitar, D. S., and Thornhill, D. P. (1973). Methimazole: Absorption, metabolism and excretion in the albino rat. *J. Pharmacol. Exp. Ther.* **184**, 432–439.

Skellern, G. G., Knight, B. I., Low, C. K., Alexander, W. D., McLarty, D. G., and Kalk, W. J. (1980). The pharmacokinetics of methimazole after oral administration of carbimazole and methimazole, in hyperthyroid patients. *Br. J. Clin. Pharmacol.* **9**, 137–143.

Stoker, T. E., Gibson, E. K., and Zorrilla, L. M. (2010). Triclosan exposure modulates estrogen-dependent responses in the female wistar rat. *Toxicol. Sci. Off. J. Soc. Toxicol.* **117**, 45–53.

Thompson, A., Griffin, P., Stuetz, R., and Cartmell, E. (2005). The fate and removal of triclosan during wastewater treatment. *Water Environ. Res.* **77**, 63–67.

Tollefsen, K. E., Scholz, S., Cronin, M. T., Edwards, S. W., de Knecht, J., Crofton, K., Garcia-Reyero, N., Hartung, T., Worth, A., and Patlewicz, G. (2014). Applying adverse outcome pathways (AOPs) to support integrated approaches to testing and assessment (IATA). *Regul. Toxicol. Pharmacol.* **70**, 629–640.

United States Environmental Protection Agency (USEPA). (1994). Reregistration eligibility decision: Sodium and zinc salts of 2-mercaptobenzothiazole. Department of Prevention, Pesticides, and Toxic Substances. 738-R-94-027. p. 168. Available at: http://archive.epa.gov/pesticides/reregistration/web/pdf/2380.pdf. Accessed December 7, 2015.

United States Environmental Protection Agency (USEPA). (2011). Exposure factors handbook. National Center for Environmental Assessment, Office of Research and Development, U. S. Environmental Protection Agency. EPA/600/R-090/052F. Available at: http://pbadupws.nrc.gov/docs/ML1400/ML14007A666.pdf. Accessed February 18, 2016.

Wambaugh, J. F., Wang, A., Dionisio, K. L., Frame, A., Egeghy, P., Judson, R., and Setzer, R. W. (2014). High throughput heuristics for prioritizing human exposure to environmental chemicals. *Environ. Sci. Technol.* **48**, 12760–12767.

Wartofsky, L., and Ingbar, S. H. (1971). Estimation of the rate of release of non-thyroxine iodine from the thyroid glands of normal subjects and patients with thyrotoxicosis. *J. Clin. Endocrinol. Metab.* **33**, 488–500.

Wu, J., Yue, H., and Cai, Z. (2009). Investigation on metabolism and pharmacokinetics of triclosan in rat plasma by using UPLC-triple quadrupole MS. *Chin. J. Chromatogr.* **27**, 724–730.

Zoeller, R. T., Tan, S. W., and Tyl, R. W. (2007). General background on the hypothalamic-pituitary-thyroid (HPT) axis. *Crit. Rev. Toxicol.* **37**, 11–53.

Zorrilla, L. M., Gibson, E. K., Jeffay, S. C., Crofton, K. M., Setzer, W. R., Cooper, R. L., and Stoker, T. E. (2009). The effects of triclosan on puberty and thyroid hormones in male Wistar rats. *Toxicol. Sci.* **107**, 56–64.